Sensory cilia as the Achilles heel of nematodes when attacked by carnivorous mushrooms

Ching-Han Lee[a,b,c], Han-Wen Chang[a,b,c], Ching-Ting Yang[a], Niaz Wali[c,d,e], Jiun-Jie Shie[c,d,e], and Yen-Ping Hsueh[a,b,c,f,1]

[a]Institute of Molecular Biology, Academia Sinica, Taipei 11529, Taiwan; [b]Molecular and Cell Biology, Taiwan International Graduate Program, Academia Sinica, Taipei 11490, Taiwan; [c]Taiwan International Graduate Program, National Defense Medical Center, Taipei 11490, Taiwan; [d]Institute of Chemistry, Academia Sinica, Taipei 11529, Taiwan; [e]Chemical Biology and Molecular Biophysics, Taiwan International Graduate Program, Academia Sinica, Taipei 10617, Taiwan; and [f]Department of Biochemical Science and Technology, National Taiwan University, Taipei 10617, Taiwan

Edited by Paul W. Sternberg, California Institute of Technology, Pasadena, CA, and approved January 27, 2020 (received for review October 22, 2019)

Fungal predatory behavior on nematodes has evolved independently in all major fungal lineages. The basidiomycete oyster mushroom *Pleurotus ostreatus* is a carnivorous fungus that preys on nematodes to supplement its nitrogen intake under nutrient-limiting conditions. Its hyphae can paralyze nematodes within a few minutes of contact, but the mechanism had remained unclear. We demonstrate that the predator–prey relationship is highly conserved between multiple *Pleurotus* species and a diversity of nematodes. To further investigate the cellular and molecular mechanisms underlying rapid nematode paralysis, we conducted genetic screens in *Caenorhabditis elegans* and isolated mutants that became resistant to *P. ostreatus*. We found that paralysis-resistant mutants all harbored loss-of-function mutations in genes required for ciliogenesis, demonstrating that the fungus induced paralysis via the cilia of nematode sensory neurons. Furthermore, we observed that *P. ostreatus* caused excess calcium influx and hypercontraction of the head and pharyngeal muscle cells, ultimately resulting in rapid necrosis of the entire nervous system and muscle cells throughout the entire organism. This cilia-dependent predatory mechanism is evolutionarily conserved in *Pristionchus pacificus*, a nematode species estimated to have diverged from *C. elegans* 280 to 430 million y ago. Thus, *P. ostreatus* exploits a nematode-killing mechanism that is distinct from widely used anthelmintic drugs such as ivermectin, levamisole, and aldicarb, representing a potential route for targeting parasitic nematodes in plants, animals, and humans.

C. elegans | oyster mushroom | predator–prey interactions | paralysis | cilia

Predators are known to evolve extraordinary adaptations to capture their prey. They employ diverse strategies, ranging from mechanical to chemical, to hunt effectively for their food. Athletic species such as leopards and cheetahs rely on their greater power and speed to catch their prey (1) whereas animals that are not athletic, such as cone snails, produce a large variety of peptide toxins that target ion channels and receptors in the neuromuscular systems of their prey (2).

Multiple fungal lineages of the Ascomycetes, Basidiomycetes, and Zygomycetes have independently evolved diverse strategies to prey on nematodes, the most abundant animals in soils (3), to supplement their nitrogen intakes. Nematode-trapping fungi such as *Arthrobotrys oligospora* (Ascomycota) and other closely related species are known to develop adhesive traps and constricting rings to mechanically catch their prey (4, 5). In contrast, the oyster mushroom *Pleurotus ostreatus* (Basidiomycota) produces chemicals to paralyze its nematode prey within a few minutes of contact (6, 7). Given the potent nematicidal activities of the *Pleurotus* species, these mushrooms may be used to control parasitic nematodes (8, 9). However, an effective management approach has not yet been established, partly because of the lack of knowledge of the basic biology of mushroom–nematode interactions in this microscopic predator–prey system. For instance, it had been unclear how *P. ostreatus* triggers paralysis in nematodes. Thus, we set out to investigate the cellular and molecular mechanisms of the *Pleurotus*-triggered paralysis in the model nematode *Caenorhabditis elegans*. We demonstrate that *P. ostreatus* paralyzes *C. elegans* via a previously unreported mechanism that is evolutionarily conserved across different nematode species. Through unbiased genetic screens, we found that the toxins produced by the *Pleurotus* mushrooms could only exert their nematicidal activity via the sensory cilia of *C. elegans*, triggering massive intracellular calcium influx and hypercontraction of the pharyngeal and body wall muscles, ultimately inducing cell necrosis in the neuromuscular system of the entire organism.

Results

***Pleurotus* Mushrooms Can Paralyze a Diversity of Nematode Species and Cause Massive Calcium Influx in *C. elegans* Pharyngeal and Body Wall Muscles.** To assess how conserved is the predator–prey interaction between *Pleurotus* mushrooms and nematodes, we tested 15 species of *Pleurotus* for their ability to paralyze *C. elegans*. We cultured *Pleurotus* species on low-nutrient medium (LNM) and directly exposed *C. elegans* to the fungal hyphae. We observed that *C. elegans* were quickly paralyzed within a few minutes of contacting the fungal hyphae (Fig. 1*A* and *SI Appendix*, Fig. S1*A*). Next, we investigated if the oyster mushroom *P. ostreatus* could paralyze a diversity of nematode species and found that nematodes of the genera *Caenorhabditis*, *Diploscapter*, *Oscheius*, *Rhabditis*, *Pristionchus*, *Panagrellus*, *Acrobeloides*, *Cephalobus*, *Mesorhabditis*, and *Pelodera* were all paralyzed and ultimately consumed (Fig. 1 *B*

Significance

Multiple fungal lineages have independently evolved carnivorous behaviors, preying on a diversity of nematodes as an adaptation for survival in low-nutrient environments. The edible oyster mushroom *Pleurotus ostreatus* is known to paralyze nematode prey, but the mechanism was unclear. We show that *P. ostreatus* triggers a massive calcium influx and rapid cell necrosis in the neuromuscular system of *C. elegans* via that nematode's sensory cilia—a mode of action that is conserved across nematodes. Our study reveals a rapid killing mechanism that has not been described previously and is distinct from that employed by common anthelmintic drugs, representing a potential route for targeting parasitic nematodes. It also establishes a paradigm for studying cell death in *C. elegans*.

Author contributions: C.-H.L. and Y.-P.H. designed research; C.-H.L., H.-W.C., C.-T.Y., and Y.-P.H. performed research; C.-H.L., H.-W.C., N.W., and J.-J.S. contributed new reagents/analytic tools; C.-H.L., H.-W.C., C.-T.Y., and Y.-P.H. analyzed data; and Y.-P.H. wrote the paper.

Competing interest statement: P.W.S. provided some materials for this work.

This article is a PNAS Direct Submission.

See online for related content such as Commentaries.

[1]To whom correspondence may be addressed. Email: pinghsueh@gate.sinica.edu.tw.

This article contains supporting information online at https://www.pnas.org/lookup/suppl/doi:10.1073/pnas.1918473117/-/DCSupplemental.

First published March 2, 2020.

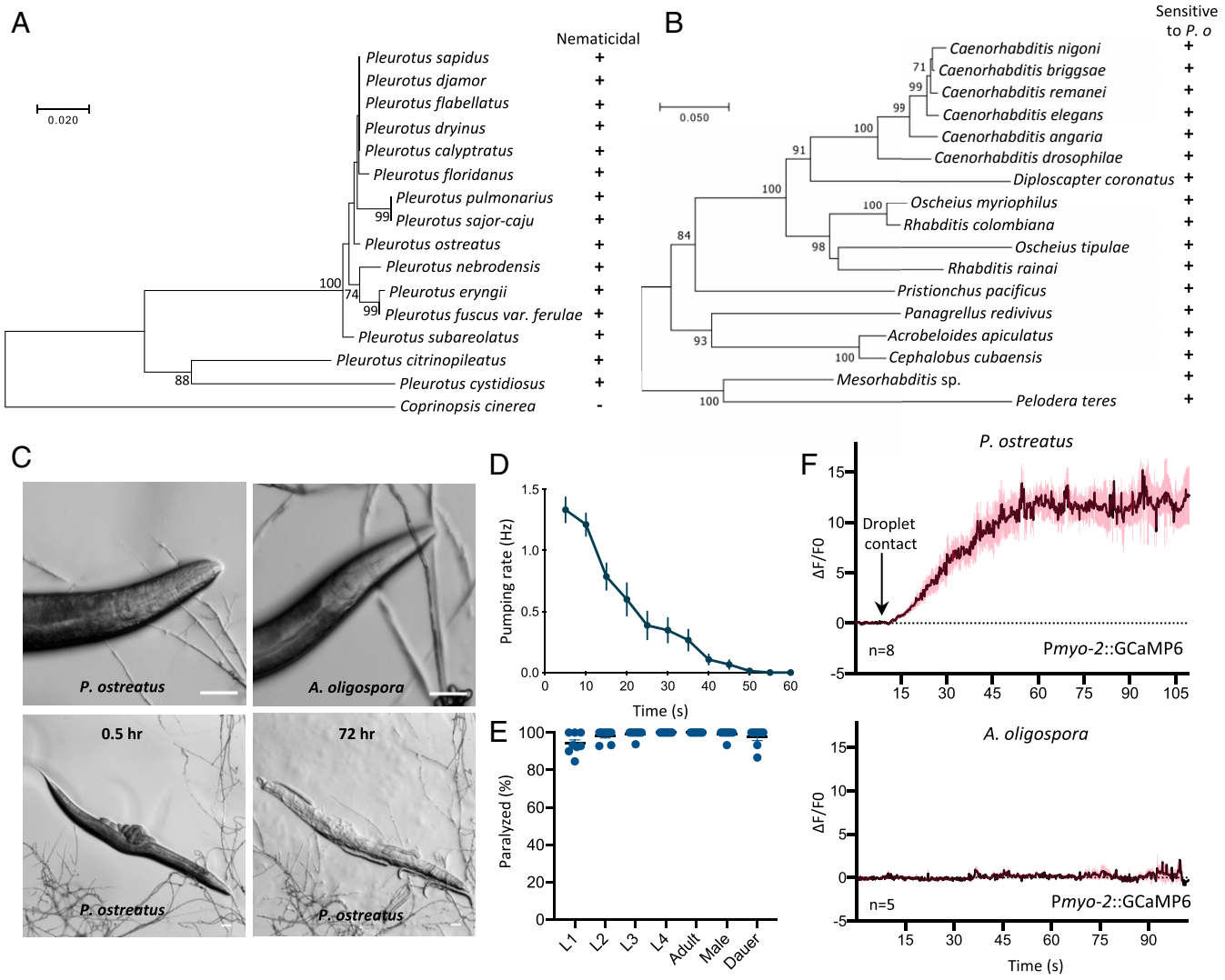

Fig. 1. *Pleurotus* mushrooms trigger paralysis and muscle hypercontraction in nematodes, including *C. elegans*. (*A*) Phylogenetic tree of the ITS region of 15 *Pleurotus* species. "+" indicates paralysis and "−" indicates no effect on *C. elegans* wild-type strain N2. *Coprinopsis cinerea* was selected as an outgroup. (*B*) Phylogenetic tree of the small-subunit rDNA regions of 17 nematode species, all of which were paralyzed by *P. ostreatus*. (*C*) Adult N2 nematode interacting with *P. ostreatus* and *A. oligospora* hyphae. (Scale bars, 50 μm.) (*D*) Pharyngeal pumping rate of adult N2 on *P. ostreatus* (mean ± SEM; $n = 15$). (*E*) Quantification of the rate of paralysis for different developmental stages of N2. Each dot represents 15 to 20 animals (mean ± SEM, $n = 8$). (*F*) GCaMP6 signal of the pharyngeal corpus of adult N2 in response to *P. ostreatus* and *A. oligospora* hyphae (mean ± SEM; *n* shown above the *x* axis).

and *C* and *SI Appendix*, Fig. S1*B*). These results demonstrate that the predator–prey relationship between *Pleurotus* fungi and nematodes is highly conserved.

We then used the model nematode *C. elegans* to dissect the molecular mechanisms underlying *P. ostreatus*-induced paralysis. When *C. elegans* came into contact with fungal hyphae, we observed marked hypercontraction of the head muscles and cessation of pharyngeal pumping. Nematodes became immobilized almost immediately after the nose of the nematode touched the spherical droplet-like structure on the fungal hyphae (Fig. 1 *C* and *D* and Movie S1). This acute paralysis response differs considerably from the outcome when *C. elegans* encounters the nematode-trapping fungus *A. oligospora*, whereby the nematodes are attracted to the fungal hyphae and continue to move for several hours after triggering fungal trap morphogenesis via their ascaroside pheromones (10, 11). We found that all developmental stages of *C. elegans* are sensitive to *P. ostreatus* and they become paralyzed upon contacting the *P. ostreatus* hyphae (Fig. 1*E*). To further characterize the observed hypercontraction of the head muscle cells and cessation of pharyngeal pumping, we expressed in *C. elegans* the calcium indicator GCaMP6 (12) under the *myo-2* and *myo-3* promoters. We found that the calcium levels were massively increased ($\Delta F/F_0 > 10$) in the corpus region of the pharynx and in the head muscles ($\Delta F/F_0 > 2.5$) upon nematodes coming into contact with the fungal hyphae (Fig. 1*F*, *SI Appendix*, Fig. S1*C*, and Movies S2 and S3).

Forward Genetic Screens Revealed That Mutants Defective in Ciliogenesis Are Resistant to *P. ostreatus*-Induced Paralysis. To gain molecular insights into the acute paralysis response of *C. elegans*, we conducted random ethyl methanesulfonate mutagenesis screens to identify *C. elegans* mutants resistant to *P. ostreatus*-induced paralysis. We conducted several rounds of mutagenesis to attain genome coverage of ∼200,000 and isolated a dozen mutants that exhibited locomotory ability on *P. ostreatus* hyphae. Quantitative measurements of the locomotion demonstrated that these mutants moved with a speed on *P. ostreatus* hyphae comparable to movements on the nonparalyzing nematode-trapping fungus

A. oligospora (Fig. 2*A* and Movie S4). To identify the mutations responsible for this phenotype, we employed single-nucleotide polymorphism (SNP) mapping (13) and whole-genome sequencing (WGS) by CloudMap (14) and identified 9 independent alleles representing loss-of-function mutations in the *C. elegans dyf-7* (15), *daf-6* (16), *osm-6* (17), *osm-1* (18), and *che-13* (19) genes (Fig. 2*B* and *SI Appendix*, Fig. S2). All of these genes have been extensively studied in *C. elegans*. *dyf-7*, *osm-6*, *osm-1*, and *che-13* are required for the development of sensory cilia, whereas *daf-6* is expressed in glial socket and sheath cells and is required for amphid channel morphogenesis (20, 21). A phenotypic hallmark of *C. elegans* mutants defective in ciliogenesis is the lack of dye uptake in the amphid sensory neurons when stained with the lipophilic dye DiI (22). Accordingly, when we applied DiI to our mutants, they failed to incorporate this fluorescent dye (Fig. 2*C*). By individually expressing the genomic fragments containing the respective wild-type genes in our mutants, we recovered their susceptibility to *P. ostreatus*-induced paralysis, as well as their ability to take up DiI dye in ciliated sensory neurons, demonstrating that resistance to fungal-induced paralysis was indeed caused by the loss-of-function mutations in these genes (Fig. 2 *C* and *D*). We further tested other *C. elegans* mutants that are known to exhibit defects in the development of ciliated sensory neurons (20)—namely the *che-11*, *daf-10*, *osm-5*, *che-2*, *dyf-2*, and *daf-19* mutants—and found that all of these mutants exhibited various degrees of resistance to the paralysis induced by contact with *P. ostreatus* hyphae (Fig. 2*E*), supporting our conclusion that intact cilia of nematode sensory neurons are required for the fungus to induce paralysis in *C. elegans*. To establish if the signaling function of these sensory neurons is required to trigger the paralysis response, we examined the sensitivity to *P. ostreatus* of mutants deficient in signaling and function of the ciliated sensory neurons. We found that mutant lines exhibiting impaired neuronal signaling (23)—such as due to mutations of the cyclic nucleotide gated channels *tax-2* and *tax-4*, G proteins *odr-3* and *gpa-3*, and transient receptor potential (TRP) channels *osm-9* and *trp-1* or the kinesin-like protein *klp-6*—were all paralyzed by *P. ostreatus* to the same extent as the wild-type nematodes (Fig. 2*E*). These results demonstrate that the structure of nematode sensory cilia must be intact for the acute paralysis response but the signaling function of the sensory cilia is

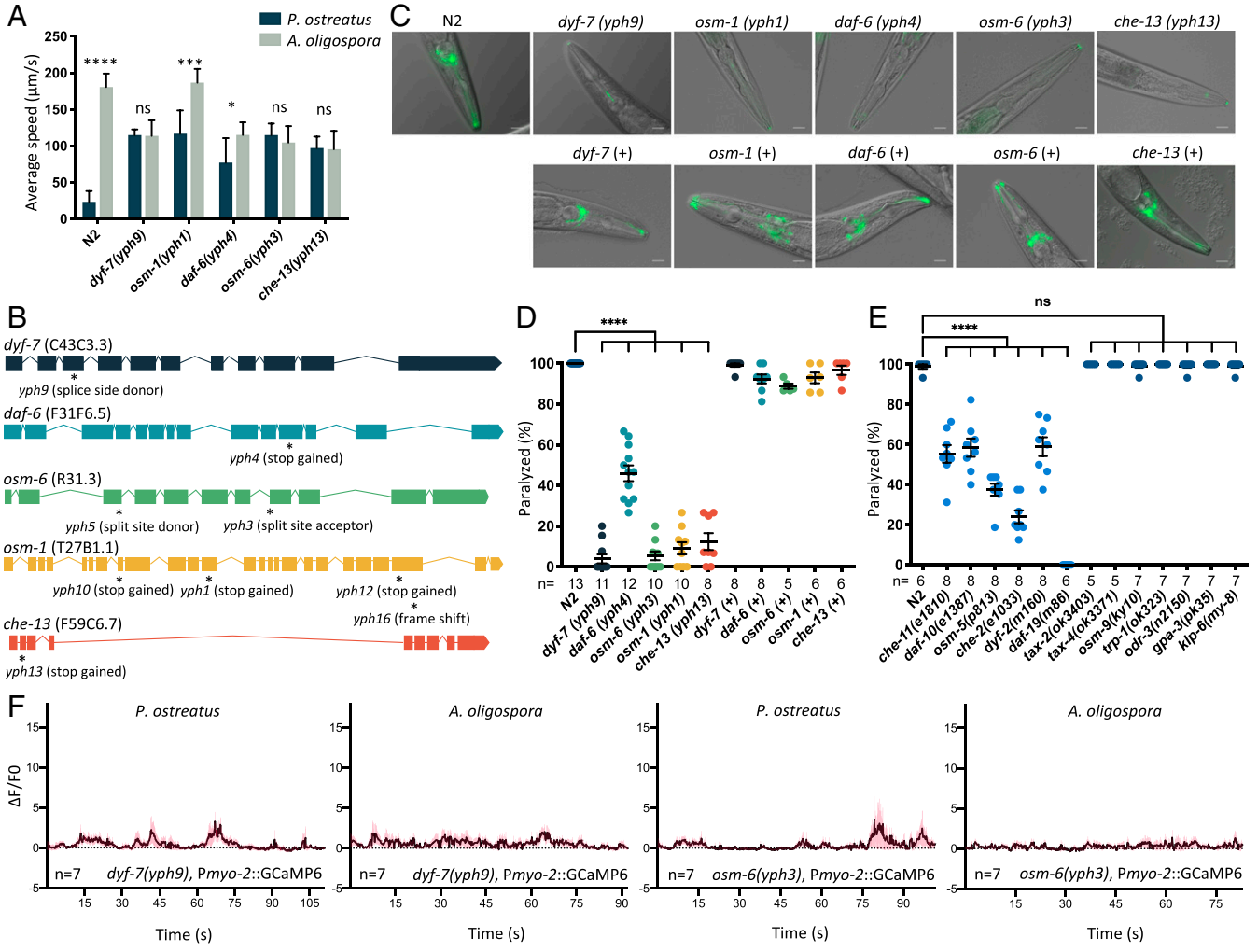

Fig. 2. Genetic screens reveal that mutants defective in ciliogenesis are resistant to *P. ostreatus*-induced paralysis. (*A*) Movement of wild-type (N2) and *P. ostreatus*-resistant *C. elegans* mutants on *P. ostreatus* and *A. oligospora* (mean ± SD; $n > 8$). (*B*) Genetic mapping and whole-genome sequencing reveal the causative mutations in *P. ostreatus*-resistant mutants (marked by asterisks). Boxes and lines represent exons and introns, respectively. (*C*) Images of DiI-stained *P. ostreatus*-resistant mutants and the respective complemented strains. (+ indicates mutants harboring the reintroduced wild-type genomic locus; *Materials and Methods*). (Scale bars, 20 μm.) (*D* and *E*) Quantification of rates of paralysis for wild-type, mutant, and complemented strains of *C. elegans* on *P. ostreatus* hyphae. Each dot represents 15 to 20 animals (mean ± SEM; *n* shown below the *x* axis). (*F*) GCaMP6 signal of the pharyngeal corpus of *P. ostreatus*-resistant mutants in response to *P. ostreatus* and *A. oligospora* hyphae (mean ± SEM; *n* shown above the *x* axis). *$P < 0.05$, ***$P < 0.001$, ****$P < 0.0001$; ns, not significant.

dispensable for responding to *P. ostreatus*. Furthermore, we also observed that the calcium level in the pharyngeal muscles of mutants resistant to *P. ostreatus*-induced paralysis (i.e., *dyf-7* and *osm-6*) did not massively increase upon hyphal contact (Fig. 2*F*).

Restoring Ciliogenesis of a Single Class of Nematode Neurons Whose Cilia Endings Are Externally Exposed Is Sufficient to Trigger Paralysis. *C. elegans* possess ~60 ciliated sensory neurons. To investigate if a single or multiple neurons are involved in triggering paralysis, we performed cell-specific rescue experiments in the *osm-6(yph3)* mutant background by using different promoters to drive expression of wild-type *osm-6* complementary (c)DNA in various neurons (Fig. 3*A* and *SI Appendix*, Fig. S3). We found that if *osm-6* expression was recapitulated in 1 or multiple head sensory neurons that have externally exposed ciliated dendritic endings (such as the IL2, ADF, ASH, and ASI neurons), the nematodes regained susceptibility to paralysis by *P. ostreatus* (Fig. 3*A*). In contrast, expressing *osm-6* in the phasmid neurons of the tail, or in the olfactory AWB and AWC neurons that are enclosed in sheath cells, failed to recover the paralysis response to *P. ostreatus* hyphae (Fig. 3*A*). We then used laser ablation to kill the IL2 and ASH neurons to determine if they are required for paralysis and found that the neuron-ablated nematodes were still sensitive to *P. ostreatus* (Fig. 3*B*). These results demonstrate that multiple ciliated sensory neurons are involved in the paralysis triggered by *P. ostreatus*, and that certain neurons possessing externally exposed ciliated dendritic endings (such as IL2) are sufficient for the paralysis response. To monitor the activity of the IL2 neurons, we expressed GCaMP6 under the *klp-6* promoter. We observed that after only 2 min of *C. elegans* touching *P. ostreatus* hyphae, there was a 2-fold increase in the GCaMP6 signals of nematode IL2 neurons (Fig. 3*C* and Movie S5), suggesting that the IL2 neurons had been activated by the fungal hyphae. However, activation of the IL2 neurons was not due to the touch response, because the GCaMP6 signal of IL2 neurons did not increase in response to touching *A. oligospora* hyphae. Furthermore, the activation of IL2 was dependent on *osm-6*, and could be complemented in a respective mutant line by expressing *osm-6* cDNA under an IL2-specific promoter (Fig. 3*D*).

Neuronal Activity Is Not Required for the Muscle Hypercontraction Triggered by *P. ostreatus*. To establish if neuronal activity is required for the phenotypes we observed when *C. elegans* encountered *P. ostreatus* hyphae, we examined head muscle hypercontraction and monitored the pharyngeal calcium levels in *tph-1* (serotonin), *cat-2* (dopamine), *eat-4* (glutamate), *unc-46* (GABA), *unc-17* (acetylcholine), *unc-13* (synaptic vesicle fusion), and *unc-31* (dense-core vesicle fusion) mutants. We found that these mutants exhibited comparable phenotypes compared with the wild-type animals, suggesting that these neurotransmitters

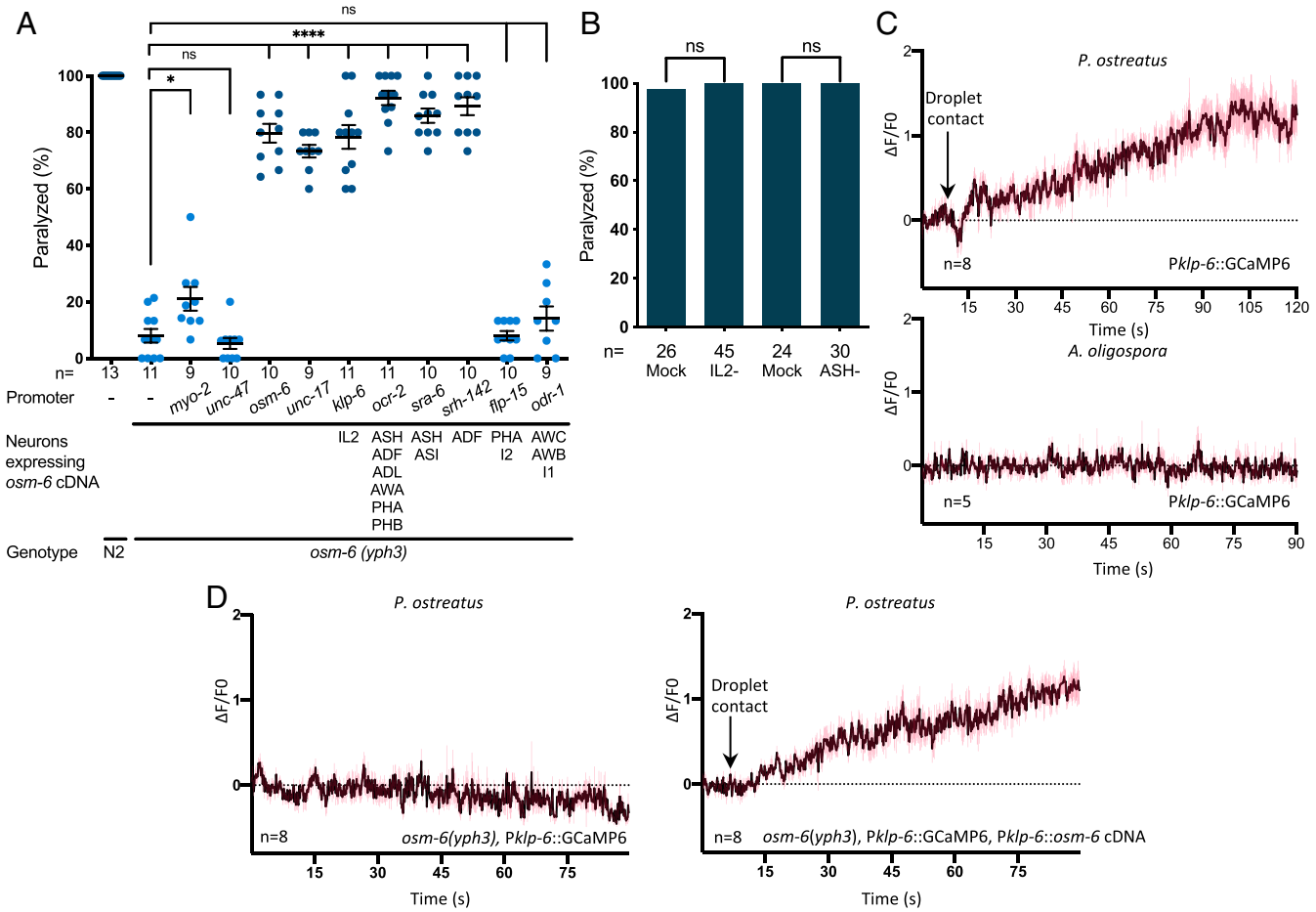

Fig. 3. Multiple ciliated sensory neurons mediate responses to *P. ostreatus* hyphae. (*A*) Quantification of the rates of paralysis in wild-type *C. elegans* (N2), the *osm-6* mutant, and cell-specific rescue lines expressing *osm-6* cDNA under various promoters (mean ± SEM; *n* shown along the *x* axis). (*B*) Quantification of *P. ostreatus*-induced paralysis in mock and laser-ablated nematodes (*n* shown along the *x* axis). (*C*) GCaMP6 signal of IL2 neurons in adult N2 in response to *P. ostreatus* or *A. oligospora* hyphae (mean ± SEM; *n* shown above the *x* axis). (*D*) GCaMP6 signal of IL2 neurons in the *osm-6* mutant (*Left*) and a cell-specific rescue line (*Right*) in response to *P. ostreatus* hyphae (mean ± SEM; *n* shown above the *x* axis). $^{*}P < 0.05$, $^{****}P < 0.0001$.

are not required for the calcium influx observed in the pharyngeal muscle cells (Fig. 4 *A* and *B*). Moreover, when we blocked synaptic transmission by expressing tetanus toxin (TeTx) in ciliated sensory neurons, we found that it did not significantly affect paralysis or the increase in pharyngeal calcium levels (Fig. 4 *C* and *D*). These results suggest that neuronal activities are dispensable for the observed calcium influx in the pharynx muscles upon contacting *Pleurotus* hyphae.

***P. ostreatus* Triggers Rapid Cell Necrosis in Multiple Tissues of *C. elegans*.** When we monitored the GCaMP6 signals in the IL2 neurons in response to contact with *P. ostreatus* hyphae, we observed that the neuronal processes became fragmented within a few minutes of exposure to the fungal hyphae. Therefore, we systematically examined different types of neurons by exposing multiple *C. elegans* neuronal reporter lines to *P. ostreatus* hyphae for 10 min and then observed the resulting neuronal morphology. Strikingly, we observed massive neuron degeneration across the entire nervous system, including of the amphid and phasmid ciliated sensory neurons, cholinergic motor neurons, mechanosensory neurons, as well as glia cells (Fig. 5*A* and Movie S6). Moreover, all developmental stages of *C. elegans* showed pronounced fragmentation of the neuronal processes and swollen cell bodies, representing morphological features of neuronal necrosis (24, 25), in all developmental stages of *C. elegans*, and this massive neuronal necrosis was independent of neurotransmission (*SI Appendix*, Fig. S4 *A* and *B*). Furthermore, the muscle cells also exhibited prominent signs of necrosis after contacting the *P. ostreatus* hyphae (Fig. 5*B*). Approximately 90% of *C. elegans* presented signs of necrosis in the head sensory neurons with externally exposed ciliated dendrites 5 min after coming into contact with *P. ostreatus* hyphae, suggesting that the fungus exerts its paralytic activity very rapidly (Fig. 5*C*). We do not consider that the observed cell death is a form of apoptosis because *ced-3* is not required (Fig. 5*D*). Next, we introduced the *Posm-6*::*GFP* reporter into the *P. ostreatus*-resistant *dyf-7*, *che-13*, and *osm-6* mutants isolated from our genetic screens, and found that the neurons were largely intact even after 10 min of exposure to *P. ostreatus* hyphae (Fig. 5*E*). We again observed massive cell necrosis when we complemented *osm-6* expression in a single class of ciliated sensory neurons (either IL2 or ADF), supporting our conclusion that the intact cilia structure of a single class of neurons is sufficient to trigger paralysis (Fig. 5*E*).

Multiple pathways can contribute to necrotic cell death in *C. elegans*. The hyperactive degenerin ion channels (26, 27) and other stress signals converge to markedly increase intracellular Ca^{2+} levels (28), signaling cell death. Since we had observed a greater than 10-fold increase in GCaMP6 signal in nematode pharyngeal muscles, we tested if this massive calcium influx is the major factor that led to cell death. To examine if the source of Ca^{2+} influx originated from the sarcoplasmic reticulum in the pharyngeal muscles, we imaged the sarcoplasmic reticulum Ca^{2+} store by expressing a low-affinity GCaMP3 variant (GCaMPer) that had been designed to attach to the lumen of the endoplasmic reticulum (ER) (29). We observed that calcium levels decreased in the sarcoplasmic reticulum upon hyphal contact (Fig. 5*F*). Furthermore, when we monitored the Pmyo2::GCaMP6 signals in the *unc-86* (ryanodine receptor) mutant background, we observed that the massively increased GCaMP signal upon hyphal contact was reduced to less than 50% of the wild-type nematodes, demonstrating that calcium influx into the pharynx was considerably diminished (Fig. 5*G*). Next, we examined if the ciliated sensory neurons and pharyngeal muscles of the *unc-68* mutant also underwent necrosis upon contact with *P. ostreatus* hyphae and found that the level of cell necrosis was comparable to that of the wild-type *C. elegans* (Fig. 5*H* and *SI Appendix*, Fig. S4*C*). In addition, cell necrosis was also not affected in the *itr-1*, *crt-1*, and *cnx-1* mutants that are known to regulate and block the necrotic cell death induced by the dominant MEC-4(d) channel (Fig. 5*H* and *SI Appendix*, Fig. S4 *C* and *D*) (30). Together, these results suggest that although the ER is the source of Ca^{2+} influx, the downstream mechanism may be distinct from previously well-characterized hyperactivated channel-mediated neurotoxicity in *C. elegans* (30).

Cilia-Dependent Paralysis by *P. ostreatus* Is Evolutionarily Conserved and the Mechanism Is Distinct from That of Known Anthelmintic Drugs. Since we observed that *P. ostreatus* could paralyze a diversity of nematode species, we wondered if the cilia-dependent mechanism is evolutionarily conserved across nematode lineages. Many genes required for ciliogenesis are highly conserved in nematodes. Therefore, we examined the *osm-1*, *dyf-2*, and *osm-3 klp20* double mutants of the nematode *Pristionchus pacificus* (31) for their response to *P. ostreatus* hyphae. *P. pacificus* diverged from *C. elegans* 280 to 430 million y ago, but we found that these *P. pacificus* mutants were also resistant to *P. ostreatus*, demonstrating that the cilia-dependent mechanism of nematode paralysis is evolutionarily conserved (Fig. 6*A* and Movie S7).

We then tested if the cilia-mediated neuronal necrosis evoked by *P. ostreatus* hyphae is a feature distinct from the effect elicited by anthelmintic drugs that can also paralyze nematodes, such as

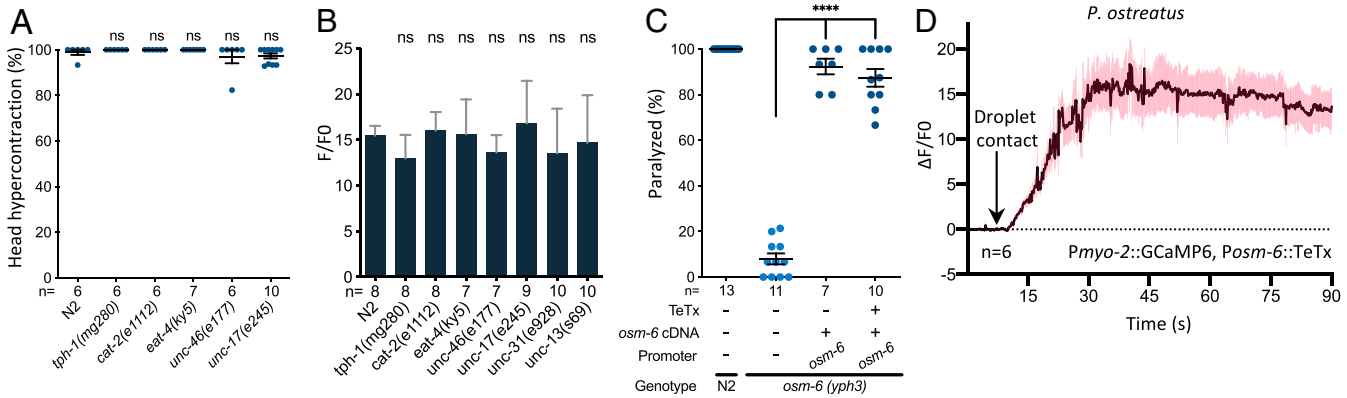

Fig. 4. Neuronal activity is not required for the paralysis induced by *P. ostreatus* hyphae. (*A*) Quantification of the head muscle hypercontraction phenotype in wild-type *C. elegans* (N2) and various neurotransmitter mutant lines (mean ± SEM; *n* shown along the *x* axis). (*B*) Quantification of the GCaMP6 signal in the pharyngeal corpus of the neurotransmitter mutant lines in response to *P. ostreatus* hyphae. (*C*) Quantification of paralysis in wild-type N2, *osm-6* mutants, and mutants expressing *osm-6* cDNA and the tetanus toxin under the *osm-6* promoter (mean ± SEM; *n* shown along the *x* axis). (*D*) GCaMP6 signal of the pharyngeal corpus in wild-type N2 expressing TeTx in ciliated sensory neurons in response to *P. ostreatus* hyphae ($n = 6$). ****$P < 0.0001$.

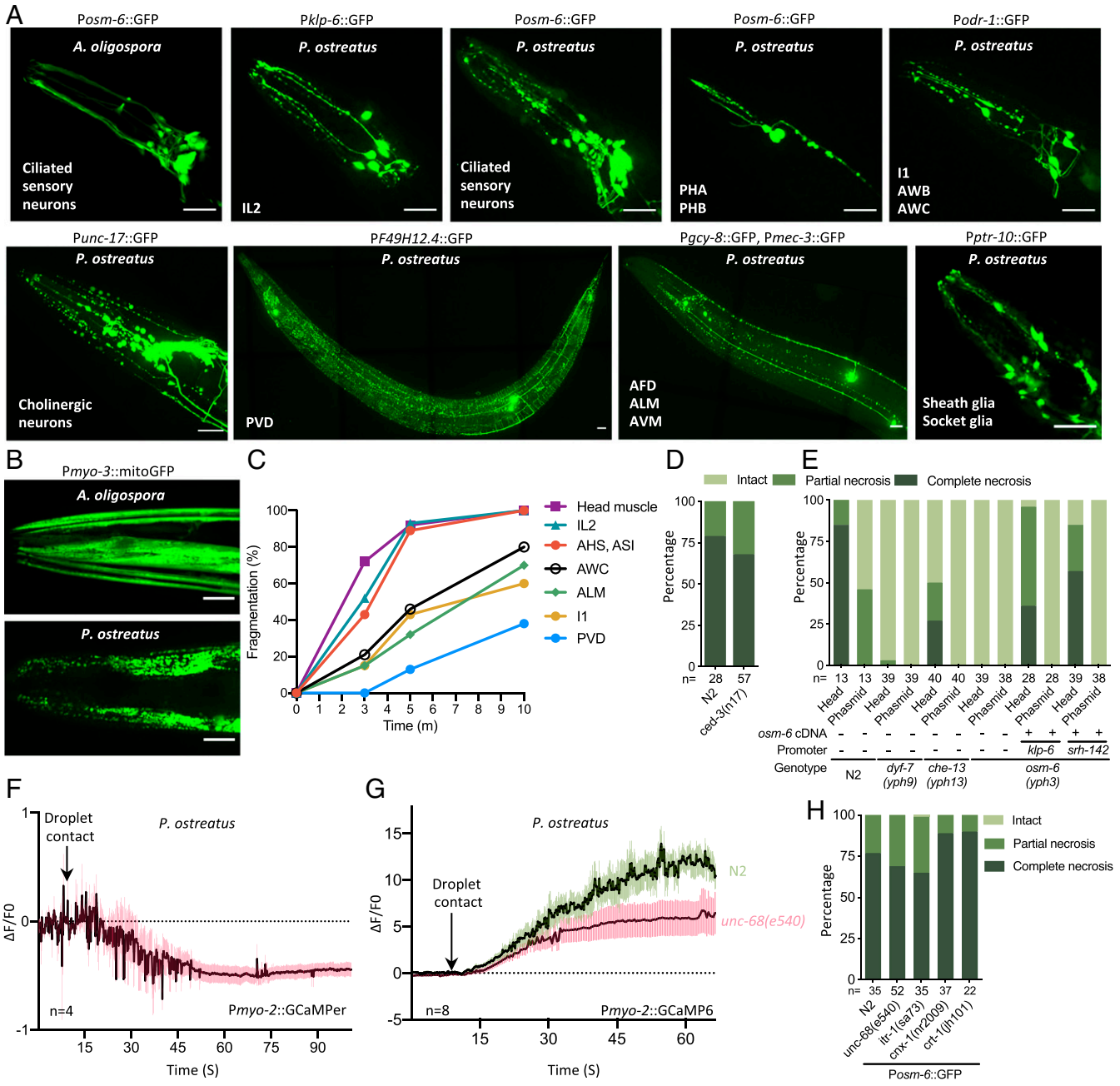

Fig. 5. *P. ostreatus* triggers rapid cell necrosis via a mechanism that requires intact ciliated sensory neurons. (*A*) Images of cell necrosis in various neurons (indicated at the bottom left of each image) and glia cells. (Scale bars, 20 μm.) (*B*) Images of cell necrosis in the head or body wall muscle (P*myo-3*::mitoGFP). (Scale bars, 20 μm.) (*C*) Rates of cell fragmentation in various reporter lines that label specific neurons and head muscle ($n > 20$ for each time point). (*D* and *E*) Quantification of necrosis of ciliated sensory neurons (P*osm-6*::GFP) in wild-type N2 and ced-3 mutants (*D*), or *Pleurotus*-resistant mutants and cell-specific rescue lines expressing *osm-6* cDNA under various promoters (*E*). (*F*) GCaMPer signal of the pharyngeal corpus of adult N2 in response to *P. ostreatus* hyphae (mean ± SEM; *n* shown above the *x* axis). (*G*) GCaMP6 signal of the pharyngeal corpus of adult N2 and *unc-68(e540)* mutants in response to *P. ostreatus* hyphae (mean ± SEM; *n* shown above the *x* axis). (*H*) Quantification of necrosis of ciliated sensory neurons in mutants in which calcium release is modulated from the ER.

ivermectin, aldicarb, and levamisole, which also paralyze *C. elegans*. Research over the past 4 decades has revealed that these anthelmintic drugs act at neuromuscular junctions (32, 33), targeting nicotinic acetylcholine receptors (levamisole) (34), glutamate-gated chloride channels (ivermectin) (35), and acetylcholinesterase (aldicarb) (36). We examined if any of these drugs cause necrosis of the ciliated sensory neurons, but there were no indications of neuronal necrosis in *C. elegans* that were paralyzed by aldicarb, levamisole, or ivermectin (Fig. 6*B*). Furthermore, when we stained the paralyzed *C. elegans* with 2′,7′-dichlorodihydrofluorescein diacetate (*H2DCFDA*), which detects reactive oxygen species (ROS), we only observed strong fluorescent signals in nematodes paralyzed upon contact with *P. ostreatus*. However, ivermectin, aldicarb, and levamisole, did not trigger ROS accumulation in the paralyzed nematodes (Fig. 6*C*). These data indicate that *P. ostreatus* paralyzes nematodes through a mechanism that is distinct from that elicited by popular anthelmintic drugs.

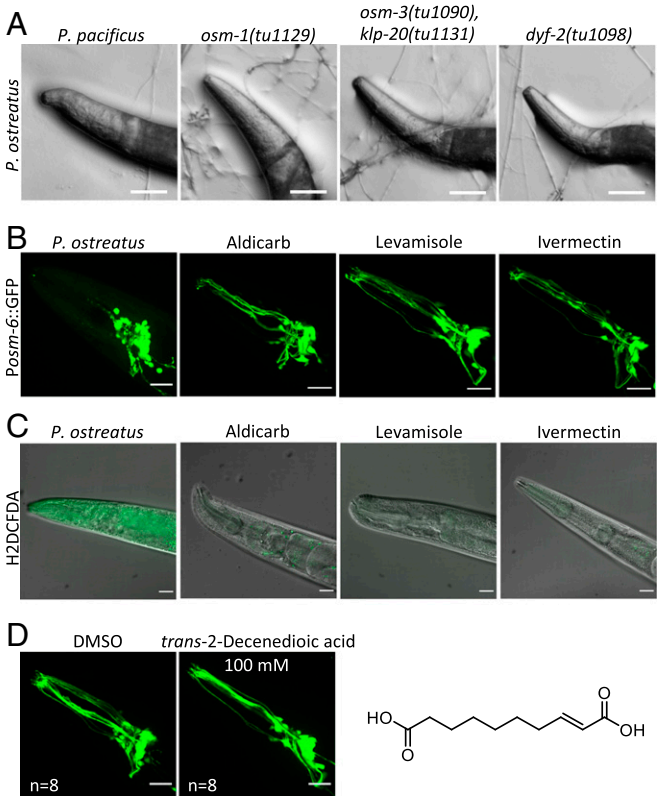

Fig. 6. Mechanism of paralysis triggered by *P. ostreatus* hyphae is evolutionarily conserved among nematodes and is distinct from that of well-known anthelmintic drugs. (*A*) Images of wild-type *P. pacificus* and cilia-defective mutants interacting with the hyphae of *P. ostreatus*. (Scale bars, 50 μm.) (*B*) Images of ciliated sensory neurons (P*osm-6*::GFP) in *C. elegans* treated with *P. ostreatus*, aldicarb, levamisole, or ivermectin. (Scale bars, 20 μm.) (*C*) Images of the head regions of paralyzed *C. elegans* stained with an indicator for reactive oxygen species (H2DCFDA). (Scale bars, 20 μm.) (*D*) Images of ciliated sensory neurons (P*osm-6*::GFP) in *C. elegans* treated with *trans*-2-decenedioic acid (100 mM) or DMSO control. (Scale bars, 20 μm.) The chemical formula of *trans*-2-decenedioic acid is also shown.

Does *P. ostreatus* produce a nematicidal toxin and what might be its chemical nature? *P. ostreatus* has been reported to produce the nematicidal toxin *trans*-2-decenedioic acid (7), and application of 330 ppm of this toxin to a population of nematodes immobilized 95% of them within an hour in vitro (7), unlike the fast-acting paralysis response of nematodes in contact with the hyphae of *P. ostreatus* in vivo. Therefore, we suspect that *P. ostreatus* produces other yet to be identified nematicidal toxins. To test if *trans*-2-decenedioic acid (7) is responsible for the paralysis phenotype we observed in *C. elegans*, we synthesized this compound and tested if it induces paralysis and neuronal necrosis. We observed that *C. elegans* locomotion was not affected even by a high concentration (100 mM) of *trans*-2-decenedioic acid and that the ciliated sensory neurons of the nematodes looked healthy (Fig. 6*D*). These results suggest that *trans*-2-decenedioic acid is not the compound produced by *P. ostreatus* responsible for rapid paralysis and systemic necrosis in *C. elegans*.

Discussion

Toxin-Induced Necrotic Responses in *C. elegans*. Many animal predators produce toxins to incapacitate their prey, and the responses of various nematodes to *Pleurotus* hyphae we present here strongly indicate that these mushrooms have independently evolved a similar strategy. Our genetic analyses clearly demonstrate that the purported toxin enters the nematode body via the sensory cilia to cause rapid and systemic necrosis in multiple tissues throughout the organism (Fig. 7). Several bacterial pathogens, including *Enterococcus faecalis*, *Photorhabdus luminescens*, and *Bacillus thuringiensis*, are known to elicit necrotic responses in *C. elegans* (37, 38). *B. thuringiensis* produces crystal pore-forming toxins that bind to glycolipids and are lethal to both nematodes and insects (39, 40). It was demonstrated recently that the crystal protein Cry6Aa triggers the necrosis pathway mediated by the aspartic protease ASP-1 (37). In the case of infections caused by *Erwinia carotovora* or *P. luminescens*, necrosis follows the bacterial infection and aggravates nematode pathology (38). These bacteria-triggered necrotic responses shared certain characteristics with the *P. ostreatus*-triggered necrosis we observed. However, *P. ostreatus*-induced necrosis occurred within minutes, whereas the bacterial infection-triggered necrosis took place only 24 h postinfection (38).

Convergent Evolution of the Predatory Fungal Mechanism Targeting Sensory Cilia of Nematode Prey. Primary cilia are sensory organelles essential for cells to sense their environments and transduce external signals (41). Studies over the past 20 y have revealed that malfunctioning cilia can give rise to many diseases (ciliopathies), and *C. elegans* has proven to be a valuable model that has contributed to our understanding of cilia biology and to the molecular basis of ciliopathies such as polycystic kidney disease and nephronophthisis (42–46). The only ciliated cell type in *C. elegans* is the sensory neuron (20). *C. elegans* have ∼60 neurons possessing diverse ciliate structures, and it is well-established that mutants exhibiting defective cilia development or function display severely compromised sensory responses, such as in chemosensation, osmosensation, mechanosensation, thermosensation, and mating (22, 43, 47). Therefore, it is likely that these mutants are inviable in nature.

Predators are known to eavesdrop on essential communication cues of their prey (48). Such strategies have evolved in animal predators, as well as carnivorous plants and fungi. For example, Venus flytraps, sundews, and pitcher plants produce fruity or flowery scents to attract their insect prey (49, 50). In our previous studies, we demonstrated that the nematode-trapping fungus *A. oligospora* not only eavesdrops on the nematode ascaroside pheromones but also lures the nematode prey by producing odorants that mimic food and sex cues that are highly attractive to many nematode species (10, 11). The chemotactic behavior of *C. elegans* depends on functional cilia and neurons so sensory cilia are also the target for nematode-trapping fungi when they seek to capture nematodes. In this study, we have demonstrated that a distinct nematicidal mechanism, which also exploits nematode sensory cilia, has independently evolved in the carnivorous oyster mushroom *P. ostreatus*. Both predatory fungi, *P. ostreatus* and *A. oligospora*, target the sensory cilia of nematodes to lure or capture their nematode prey.

Future Applications of *P. ostreatus* Treatment for Parasitic Nematode Control. In recent years, anthelmintic resistance has become a major global problem for controlling livestock parasites and has also been observed in patients suffering from river blindness (51, 52). Thus, new anthelmintic compounds with novel mechanisms of action are urgently required. Our results demonstrate that the hyphae of *P. ostreatus* can paralyze nematodes via a mechanism that is distinct from those of several currently available anthelmintics, including ivermectin, which is the most widely used antiparasitic drug in human and veterinary medicine (53). Furthermore, since *P. ostreatus* is highly effective against a wide range of nematode species, we believe that the paralysis-inducing agent produced by *P. ostreatus* has far-reaching potential as a novel type of drug that could be used in the future to target the parasitic nematodes of plants, animals, and humans.

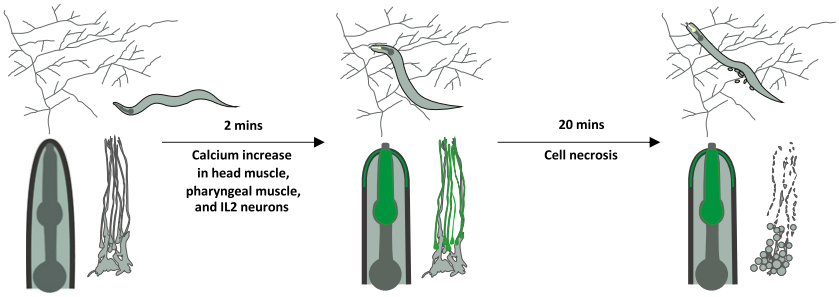

Fig. 7. Contact with *P. ostreatus* hyphae induces massive cell calcium influx and cell necrosis in nematodes via ciliated sensory neurons.

Materials and Methods

Strains. Nematode strains were maintained at room temperature on nematode growth medium plates seeded with *Escherichia coli*, OP50. Transgenic animals were generated using standard microinjection techniques (54). Fungal cultures were grown on potato dextrose agar (Difco) or low-nutrient mineral salts medium (2% agar, 1.66 mM $MgSO_4$, 5.4 μM $ZnSO_4$, 2.6 μM $MnSO_4$, 18.5 μM $FeCl_3$, 13.4 mM KCl, 0.34 μM biotin, and 0.75 μM thiamin). The nematode and fungal strains used in this study and their sources are listed in *SI Appendix*.

Genetic Screen, Single-Nucleotide Polymorphism Mapping, and Whole-Genome Sequencing. Ethyl methanesulfonate mutagenesis was conducted following a standard protocol (55). Semisynchronized F2 populations were screened on *P. ostreatus* cultures. Mutants that exhibited a resistant phenotype were singled out and their progeny were subjected to rescreening. Approximately 200,000 genomes were screened, and ∼30 mutants were isolated. Nine mutants which exhibited a strong resistant phenotype were subjected to further genetic mapping and WGS. Rapid SNP mapping with the Hawaiian strain was conducted as described (13). Genomic DNA was extracted from the F2 progeny of the mutant and Hawaiian crosses and subjected to Illumina WGS at 11× to 13× depth of coverage. WGS data were analyzed using the CloudMap pipeline (14).

***C. elegans* Response Assays.** *C. elegans* locomotion was recorded and analyzed using WormLab (MBF Bioscience). One-day-old adult hermaphrodites were transferred to 14-d LNM cultures of *P. ostreatus* and *A. oligospora*. After 10 min of fungal exposure, their behavior was recorded for 2 min. To quantify the rate of paralysis, 15 to 20 adult animals were transferred to *P. ostreatus* for 10 min. Hypercontraction of the head muscles and cessation of pharyngeal pumping defined the paralysis phenotype. To assess the *C. elegans* pumping rate in contact with *P. ostreatus*, 1-d-old adult N2 individuals were placed on *P. ostreatus* and the pumping rate was scored by eye using a stereo dissecting microscope (Nikon; SMZ745). The pumping rate was determined by the number of pumping events every 5 s.

Calcium Imaging. Transgenic animals expressing GCaMP6 under various promoters were transferred to *P. ostreatus* or *A. oligospora* cultures and the calcium responses were recorded with a Zeiss SteREO V20 microscope with an Andor Zyla 5.5 sCMOS camera. The fluorescence intensity of the region of interest (ROI) was automatically drawn and analyzed via a customized module in MetaXpress. F is the fluorescence intensity of the ROI-subtracted background fluorescence. F_0 is the average F of ∼80 frames at the beginning of the video.

Cell-Specific Rescue. *osm-6* cDNA was PCR-amplified from N2 cDNA, subcloned into a pSM plasmid using the In-Fusion HD Cloning Kit (Takara). Various promoter sequences were further subcloned into the plasmid using SphI and AscI. The plasmids were injected into the *osm-6* mutant (*yph3*) background. One-day-old adults of the transgenic animals were subjected to *C. elegans* response assay and dye-filling assay.

Neuronal Necrosis Assay. Nematodes were transferred to *P. ostreatus* or *A. oligospora* for 10 min, and subjected to a 3% agar pad on glass slides with 500 mM NaN_3. The neuronal necrosis phenotype was quantified and imaged by compound microscopy 20 min later. To image the neuronal necrosis, the nematodes were analyzed with an Andor Revolution WD with a Nikon Ti-E automatic microscope with a Lambda 60× oil lens. Images were captured with an iXon Ultra 888 EMCCD (Andor), and analyzed with MetaMorph.

Statistics. Two-tailed Student's t test was performed to determine the statistical difference between the control and remaining samples using GraphPad Prism 8. In the figures, asterisks denote statistical significance as calculated by Student's t test ($^*P < 0.05$, $^{**}P < 0.01$, $^{***}P < 0.001$, $^{****}P < 0.0001$).

Data Availability. All data are available in the article, the *SI Appendix*, and Movies S1–S7. Additional methods can be found in *SI Appendix, Materials and Methods*.

ACKNOWLEDGMENTS. We thank the Caenorhabditis Genetic Center (CGC), WormBase, P.W.S., Chun-Liang Pan, Yi-Chun Wu, and Ralf Sommer for sharing the nematode strains; and the Bioresource Collection and Research Center, Sung-Yuan Hsieh, and Ursula Kües for sharing the fungal strains. We thank Brandon Harvey for providing the GCaMPer construct. We are grateful to Chun-Liang Pan, John O'Brien, and Meng-Chao Yao for their comments and suggestions on the manuscript; and for the technical assistance of Ling-Mei Hsu and A-Mei Yang in the laboratory. We thank Ching-Che Lee for designing the graphic model. The CGC is funded by the NIH Office of Research Infrastructure Programs (P40 OD010440). This work was supported by Academia Sinica Career Development Award AS-CDA-106-L03 and the Foundation for the Advancement of Outstanding Scholarship Young Scholars' Creativity Award (to Y.-P.H.).

1. A. M. Wilson *et al.*, Biomechanics of predator-prey arms race in lion, zebra, cheetah and impala. *Nature* **554**, 183–188 (2018).
2. B. M. Olivera *et al.*, Peptide neurotoxins from fish-hunting cone snails. *Science* **230**, 1338–1343 (1985).
3. J. van den Hoogen *et al.*, Soil nematode abundance and functional group composition at a global scale. *Nature* **572**, 194–198 (2019).
4. B. Nordbring-Hertz, Nematophagous fungi: Strategies for nematode exploitation and for survival. *Microbiol. Sci.* **5**, 108–116 (1988).
5. G. L. Barron, *The Nematode-Destroying Fungi* (Canadian Biological Publications, 1977).
6. R. G. Thorn, G. L. Barron, Carnivorous mushrooms. *Science* **224**, 76–78 (1984).
7. O. C. H. Kwok, R. Plattner, D. Weisleder, D. T. Wicklow, A nematicidal toxin from *Pleurotus ostreatus* NRRL 3526. *J. Chem. Ecol.* **18**, 127–136 (1992).
8. M. H. Hahn, L. L. M. De Mio, O. J. Kuhn, H. D. S. Duarte, Nematophagous mushrooms can be an alternative to control *Meloidogyne javanica*. *Biol. Control* **138**, 104024 (2019).
9. C. C. Okorie, C. C. Ononuju, I. A. Okwujiako, Management of *Meloidogyne incognita* with *Pleurotus ostreatus* and *P. tuberregium* in soybean. *Int. J. Agric. Biol.* **13**, 401–405 (2011).
10. Y. P. Hsueh, P. Mahanti, F. C. Schroeder, P. W. Sternberg, Nematode-trapping fungi eavesdrop on nematode pheromones. *Curr. Biol.* **23**, 83–86 (2013).
11. Y. P. Hsueh *et al.*, Nematophagous fungus *Arthrobotrys oligospora* mimics olfactory cues of sex and food to lure its nematode prey. *eLife* **6**, e20023 (2017).
12. T. W. Chen *et al.*, Ultrasensitive fluorescent proteins for imaging neuronal activity. *Nature* **499**, 295–300 (2013).
13. M. W. Davis *et al.*, Rapid single nucleotide polymorphism mapping in *C. elegans*. *BMC Genom.* **6**, 118 (2005).
14. G. Minevich, D. S. Park, D. Blankenberg, R. J. Poole, O. Hobert, CloudMap: A cloud-based pipeline for analysis of mutant genome sequences. *Genetics* **192**, 1249–1269 (2012).
15. M. G. Heiman, S. Shaham, DEX-1 and DYF-7 establish sensory dendrite length by anchoring dendritic tips during cell migration. *Cell* **137**, 344–355 (2009).
16. E. A. Perens, S. Shaham, *C. elegans daf-6* encodes a patched-related protein required for lumen formation. *Dev. Cell* **8**, 893–906 (2005).
17. J. Collet, C. A. Spike, E. A. Lundquist, J. E. Shaw, R. K. Herman, Analysis of *osm-6*, a gene that affects sensory cilium structure and sensory neuron function in *Caenorhabditis elegans*. *Genetics* **148**, 187–200 (1998).

18. L. R. Bell, S. Stone, J. Yochem, J. E. Shaw, R. K. Herman, The molecular identities of the *Caenorhabditis elegans* intraflagellar transport genes *dyf-6*, *daf-10* and *osm-1*. *Genetics* **173**, 1275–1286 (2006).
19. C. J. Haycraft, J. C. Schafer, Q. Zhang, P. D. Taulman, B. K. Yoder, Identification of CHE-13, a novel intraflagellar transport protein required for cilia formation. *Exp. Cell Res.* **284**, 251–263 (2003).
20. P. N. Inglis, G. Ou, M. R. Leroux, J. M. Scholey, The sensory cilia of *Caenorhabditis elegans*. *WormBook*, 1–22 (2007).
21. G. Oikonomou *et al*., Opposing activities of LIT-1/NLK and DAF-6/patched-related direct sensory compartment morphogenesis in *C. elegans*. *PLoS Biol.* **9**, e1001121 (2011).
22. L. A. Perkins, E. M. Hedgecock, J. N. Thomson, J. G. Culotti, Mutant sensory cilia in the nematode *Caenorhabditis elegans*. *Dev. Biol.* **117**, 456–487 (1986).
23. C. I. Bargmann, Chemosensation in *C. elegans*. *WormBook*, 1–29 (2006).
24. D. H. Hall *et al*., Neuropathology of degenerative cell death in *Caenorhabditis elegans*. *J. Neurosci.* **17**, 1033–1045 (1997).
25. V. Nikoletopoulou, N. Tavernarakis, Necrotic cell death in *Caenorhabditis elegans*. *Methods Enzymol.* **545**, 127–155 (2014).
26. M. Driscoll, M. Chalfie, The mec-4 gene is a member of a family of *Caenorhabditis elegans* genes that can mutate to induce neuronal degeneration. *Nature* **349**, 588–593 (1991).
27. M. Chalfie, E. Wolinsky, The identification and suppression of inherited neurodegeneration in *Caenorhabditis elegans*. *Nature* **345**, 410–416 (1990).
28. N. Kourtis, N. Tavernarakis, Non-developmentally programmed cell death in *Caenorhabditis elegans*. *Semin. Cancer Biol.* **17**, 122–133 (2007).
29. M. J. Henderson *et al*., A low affinity GCaMP3 variant (GCaMPer) for imaging the endoplasmic reticulum calcium store. *PLoS One* **10**, e0139273 (2015).
30. K. Xu, N. Tavernarakis, M. Driscoll, Necrotic cell death in *C. elegans* requires the function of calreticulin and regulators of Ca(2+) release from the endoplasmic reticulum. *Neuron* **31**, 957–971 (2001).
31. E. Moreno *et al*., Regulation of hyperoxia-induced social behaviour in *Pristionchus pacificus* nematodes requires a novel cilia-mediated environmental input. *Sci. Rep.* **7**, 17550 (2017).
32. S. M. Blazie, Y. Jin, Pharming for genes in neurotransmission: Combining chemical and genetic approaches in *Caenorhabditis elegans*. *ACS Chem. Neurosci.* **9**, 1963–1974 (2018).
33. L. Holden-Dye, R. J. Walker, Anthelmintic drugs and nematicides: Studies in *Caenorhabditis elegans*. *WormBook*, 1–29 (2014).
34. J. A. Lewis, C. H. Wu, H. Berg, J. H. Levine, The genetics of levamisole resistance in the nematode *Caenorhabditis elegans*. *Genetics* **95**, 905–928 (1980).
35. J. A. Dent, M. M. Smith, D. K. Vassilatis, L. Avery, The genetics of ivermectin resistance in *Caenorhabditis elegans*. *Proc. Natl. Acad. Sci. U.S.A.* **97**, 2674–2679 (2000).
36. M. Nguyen, A. Alfonso, C. D. Johnson, J. B. Rand, *Caenorhabditis elegans* mutants resistant to inhibitors of acetylcholinesterase. *Genetics* **140**, 527–535 (1995).
37. F. Zhang *et al*., *Bacillus thuringiensis* crystal protein Cry6Aa triggers *Caenorhabditis elegans* necrosis pathway mediated by aspartic protease (ASP-1). *PLoS Pathog.* **12**, e1005389 (2016).
38. D. Wong, D. Bazopoulou, N. Pujol, N. Tavernarakis, J. J. Ewbank, Genome-wide investigation reveals pathogen-specific and shared signatures in the response of *Caenorhabditis elegans* to infection. *Genome Biol.* **8**, R194 (2007).
39. J. S. Griffitts *et al*., Glycolipids as receptors for *Bacillus thuringiensis* crystal toxin. *Science* **307**, 922–925 (2005).
40. M. Cappello *et al*., A purified *Bacillus thuringiensis* crystal protein with therapeutic activity against the hookworm parasite *Ancylostoma ceylanicum*. *Proc. Natl. Acad. Sci. U.S.A.* **103**, 15154–15159 (2006).
41. M. V. Nachury, D. U. Mick, Establishing and regulating the composition of cilia for signal transduction. *Nat. Rev. Mol. Cell Biol.* **20**, 389–405 (2019).
42. A. R. Jauregui, K. C. Q. Nguyen, D. H. Hall, M. M. Barr, The *Caenorhabditis elegans* nephrocystins act as global modifiers of cilium structure. *J. Cell Biol.* **180**, 973–988 (2008).
43. M. M. Barr, P. W. Sternberg, A polycystic kidney-disease gene homologue required for male mating behaviour in *C. elegans*. *Nature* **401**, 386–389 (1999).
44. P. Sengupta, Cilia and sensory signaling: The journey from "animalcules" to human disease. *PLoS Biol.* **15**, e2002240 (2017).
45. I. V. Nechipurenko, P. Sengupta, The rise and fall of basal bodies in the nematode *Caenorhabditis elegans*. *Cilia* **6**, 9 (2017).
46. J. Wang *et al*., *C. elegans* ciliated sensory neurons release extracellular vesicles that function in animal communication. *Curr. Biol.* **24**, 519–525 (2014).
47. C. I. Bargmann, E. Hartwieg, H. R. Horvitz, Odorant-selective genes and neurons mediate olfaction in *C. elegans*. *Cell* **74**, 515–527 (1993).
48. B. M. Siemers, E. Kriner, I. Kaipf, M. Simon, S. Greif, Bats eavesdrop on the sound of copulating flies. *Curr. Biol.* **22**, R563–R564 (2012).
49. A. Jurgens, A. M. El-Sayed, D. M. Suckling, Do carnivorous plants use volatiles for attracting prey insects? *Funct. Ecol.* **23**, 875–887 (2009).
50. B. Di Giusto *et al*., Flower-scent mimicry masks a deadly trap in the carnivorous plant *Nepenthes rafflesiana*. *J. Ecol.* **98**, 845–856 (2010).
51. R. M. Kaplan, A. N. Vidyashankar, An inconvenient truth: Global worming and anthelmintic resistance. *Vet. Parasitol.* **186**, 70–78 (2012).
52. M. Y. Osei-Atweneboana *et al*., Phenotypic evidence of emerging ivermectin resistance in *Onchocerca volvulus*. *PLoS Negl. Trop. Dis.* **5**, e998 (2011).
53. R. Laing, V. Gillan, E. Devaney, Ivermectin—Old drug, new tricks? *Trends Parasitol.* **33**, 463–472 (2017).
54. C. C. Mello, J. M. Kramer, D. Stinchcomb, V. Ambros, Efficient gene transfer in *C. elegans*: Extrachromosomal maintenance and integration of transforming sequences. *EMBO J.* **10**, 3959–3970 (1991).
55. L. M. Kutscher, S. Shaham, Forward and reverse mutagenesis in *C. elegans*. *WormBook*, 1–26 (2014).